Silica-supported ZnS.cntdot.CdS mixed semiconductor catalysts for photogeneration of hydrogen

A. Ueno, N. Kakuta, K. H. Park, M. F. Finlayson, A. J. Bard, A. Campion, M. A. Fox, S. E. Webber, and J. M. White

J. Phys. Chem., **1985**, 89 (18), 3828-3833 • DOI: 10.1021/j100264a012

In an attempt to provide further confirmation of the conformational model, we are presently carrying out similar experiments with symmetrically substituted bipyridyl derivatives. It is our hope that with the appropriate choice of substituent and its position on the bipyridyl molecule, we would be able to constrain the rotational freedom of the molecule such that it would be forced to exist in only a single conformation. Observation of only one set of ODMR transitions in such a case would clearly favor the interpretation of two conformations.

Acknowledgment. Acknowledgment is made to the donors of the Petroleum Research Fund, administered by the American Chemical Society, for partial support of this work, to the University of Vermont (UVM PS-11), and to the Research Corporation (9326).

Registry No. Bipyridyl, 366-18-7.

Silica-Supported ZnS·CdS Mixed Semiconductor Catalysts for Photogeneration of Hydrogen

A. Ueno,† N. Kakuta, K. H. Park, M. F. Finlayson, A. J. Bard, A. Campion, M. A. Fox, S. E. Webber, and J. M. White*

Department of Chemistry, University of Texas, Austin, Texas 78712 *(Received: February 26, 1985)*

A silica-supported mixed semiconductor catalyst, ZnS·CdS/SiO_2, immersed in aqueous sulfide solutions shows significant activity for hydrogen generation from water under illumination with either UV or visible light. The individually supported ZnS/SiO_2 and CdS/SiO_2 were much less active. A physical mixture of ZnS/SiO_2 and CdS/SiO_2 also did not improve the activity, even when the amounts of ZnS and CdS were the same as those in the ZnS·CdS/SiO_2 catalyst. This indicates that intimate contact between ZnS and CdS particles is necessary for photogeneration of hydrogen. Surface analysis (X-ray photoelectron spectroscopy and sputtering) indicates that the active catalyst had a layered structure around the silica particles with a CdS-rich layer coating the silica and a ZnS-rich layer overcoating the CdS. Samples prepared by sequential deposition of ZnS followed by CdS were much less active for hydrogen production than samples prepared either by sequential deposition in the opposite order or by coprecipitation. ZnS·CdS on a number of other supports (e.g. Nafion, nylon, and alumina) is also quite active. Electron microscopy and X-ray diffraction show that neither bulk particle morphology nor support are critical. Overall, the critical factors are (1) CdS overcoating ZnS, (2) close proximity of Cds and ZnS, and (3) minimization of particle shadowing (light scattering).

Introduction

Photogeneration of hydrogen from water is of current interest and has been extensively studied by using semiconductors as optically active materials. Oxide semiconductors such as TiO_2[1] and $SrTiO_3$[2] have been attractive because of their stability with respect to photodriven corrosion. Chalcogenide semiconductors have also been used but require sacrificial reagents such as Na_2S and Na_2SO_3 to limit photocorrosion.[3] Among the chalcogenides, zinc[4] and cadmium[5] sulfides have been widely studied and their electronic and electrochemical properties are reasonably well described.

Light conversion efficiencies of these semiconductor materials increase with increasing surface-to-volume ratios. Henglein et al.[6,7] studied the electronic properties and activities for photogeneration of hydrogen using *colloidal* ZnS and CdS. They reported that the electronic structure of these colloidal chalcogenides differed from that of larger particles. This was reflected in a shorter wavelength onset of the absorption spectra of the colloids. Reber et al.[8] have also reported an enhancement in the rate of hydrogen generation as the particle size decreased to colloidal dimensions. Gratzel et al.[9] proposed an interparticle electron transfer to explain an enhancement in the rate of hydrogen production with a CdS/TiO_2 mixed semiconductor system. In earlier work we have shown that a ZnS·CdS mixed semiconductor catalyst incorporated into a Nafion film is a factor of 50 more active for photogeneration of hydrogen than either ZnS/Nafion or CdS/Nafion.[10]

The purpose of the present work was to study the morphology/structure of a ZnS·CdS mixed semiconductor catalyst on SiO_2 and to compare these results with other supports, including Nafion.[10]

† Present address: Department of Materials Science, Toyohashi University of Technology, Toyohashi 440, Japan.

Experimental Section

(1) Catalyst Preparation. Several kinds of catalysts composed of ZnS and/or CdS were employed and their preparation procedures are given in the following paragraphs.

(a) ZnS/SiO_2 and CdS/SiO_2. The ZnS and CdS catalysts were prepared by conventional impregnation techniques. Silica powder (1.00 g of Cab-O-Sil 300, Degussa) was immersed in 50 mL of aqueous solution containing 2.3×10^{-3} mol of $Zn(NO_3)_2 \cdot 6H_2O$ (Fisher Scientific) or $Cd(NO_3)_2 \cdot 4H_2O$ (Fisher Scientific). The mixture was stirred for 2 h and then 50 mL of water saturated

(1) S. N. Frank and A. J. Bard, *J. Phys. Chem.*, **81**, 1484 (1977); A. J. Bard, *J. Photochem.*, **10**, 59 (1979); T. Sakata and T. Kawai, *Chem. Phys. Lett.*, **80**, 341 (1981).
(2) J.-M. Lehn, J.-P. Sauvage, and R. Ziessel, *Nouv. J. Chim.*, **4**, 623 (1980); K. Domen, S. Naito, T. Onishi, and K. Tamaru, *Chem. Phys. Lett.*, **92**, 433 (1982).
(3) T. Inoue, T. Watanabe, A. Fujishima, K. Honda, and K. Kobayakawa, *J. Electrochem. Soc.*, **124**, 719 (1977); A. B. Ellis, S. W. Kaiser, and M. S. Wrighton, *J. Am. Chem. Soc.*, **98**, 6855 (1976).
(4) R. E. Stephens, B. Ke, and D. Trivich, *J. Phys. Chem.*, **59**, 966 (1976), S. Yanagida, T. Azuma, and H. Sakurai, *Chem. Lett.*, 1868 (1982).
(5) M. Gutierrez and A. Henglein, *Ber. Bunsenges. Phys. Chem.*, **87**, 474 (1983); J. R. Darwent, *J. Chem. Soc., Faraday Trans. 2*, **77**, 1703 (1981); M. Matsumura, Y. Saho, and H. Tsubomura, *J. Phys. Chem.*, **87**, 3807 (1983).
(6) A. Henglein and M. Gutierrez, *Ber. Bunsenges. Phys. Chem.*, **87**, 852 (1983).
(7) H. Weller, U. Koch, M. Gutierrez, and A. Henglein, *Ber. Bunsenges. Phys. Chem.*, **88**, 649 (1984).
(8) J.-F. Reber and K. Meier, *J. Phys. Chem.*, **88**, 5903 (1984).
(9) N. Serpone, E. Borgarello, and M. Gratzel, *J. Chem. Soc., Chem. Commun.*, 342 (1984); E. Borgarello, K. Kalyanasundarama, and M. Gratzel, *Helv. Chim. Acta*, **65**, 243 (1982).
(10) N. Kakuta, K.-H. Park, M. F. Finlayson, A. J. Bard, A. Campion, M. A. Fox, S. E. Webber, and J. M. White *J. Phys. Chem.*, **89**, 732 (1985); A. W.-H. Mau, C. B. Huang, N. Kakuta, A. J. Bard, A. Campion, M. A. Fox, J. M. White, and S. E. Webber, *J. Am. Chem. Soc.*, **106**, 6537 (1984).

0022-3654/85/2089-3828$01.50/0

with H_2S was added. Stirring continued for an additional 24 h. The resultant precipitates were filtered and dried in an oven at 110 °C. The powders thus obtained were 24 wt % ZnS and 26 wt % CdS, as determined by atomic absorption spectroscopy. A physical mixture of these two (mixing ratio 1:1 by weight) was often used in this work and is denoted $ZnS/SiO_2 + CdS/SiO_2$.

(*b*) *ZnS·CdS/SiO₂ Catalysts.* The catalyst used for most of this work was prepared by impregnation of 1.00 g of SiO_2 powder with 50 mL of water containing 1.15×10^{-3} mol each of $Zn(NO_3)_2 \cdot 6H_2O$ and $Cd(NO_3)_2 \cdot 4H_2O$. The other procedures are the same as those described above. Atomic absorption spectroscopic analysis gave the amounts of ZnS and CdS as 11 and 17 wt %, respectively. In another set of catalysts, the atomic ratio of Cd/Zn in $ZnS \cdot CdS/SiO_2$ was varied by changing the concentration of $Cd(NO_3)_2 \cdot 4H_2O$ while keeping the $Zn(NO_3)_2 \cdot 6H_2O$ concentration constant. In a third set of experiments, the total loading of ZnS and CdS was varied from 12.5 to 75 wt %, keeping the Cd/Zn atomic ratio equal to unity.

(*c*) *ZnS(CdS/SiO₂) and CdS(ZnS/SiO₂) Catalysts.* These catalysts were designed to be composed of ZnS and CdS layers around the SiO_2 powder particles. The $ZnS(CdS/SiO_2)$ catalyst was prepared by impregnation of 1.00 g of SiO_2 powder with 50 mL of water containing 1.15×10^{-3} mol of $Cd(NO_3)_2 \cdot 4H_2O$, followed by the addition of 50 mL of H_2S-saturated water with stirring for 24 h. Then 50 mL of water containing 1.15×10^{-3} mol of $Zn(NO_3)_2 \cdot 6H_2O$ was poured into the solution, followed by another 50 mL of H_2S-saturated water with stirring for an additional 24 h. In the case of the $CdS(ZnS/SiO_2)$ catalyst, the preparation procedure was reversed to give CdS concentrated in the outermost layer.

(*d*) *Unsupported ZnS·CdS Catalyst.* This catalyst was prepared by coprecipitation, using H_2S, of ZnS and CdS particles from an aqueous solution containing equimolar amounts of $Zn(NO_3)_2 \cdot 6H_2O$ and $Cd(NO_3)_2 \cdot 4H_2O$ but no silica.

(*e*) *ZnS·CdS/Other Supports.* A variety of supports other than SiO_2 were investigated. These included Nafion films (Nafion 111, 30 μm thick, and Nafion 117, 180 μm thick), frosted glass (Scientific Products Microslides M6147), weighing paper (VWR Scientific no. 12578-201), nylon mesh (40 μm strand diameter, 75 μm strand spacing), 3-μm Al_2O_3 films, and colloids obtained from sonication of ZnS·CdS nylon.

In all cases, the substrate was soaked in a 0.5 M $Cd(NO_3)_2$–0.5 M $Zn(nNO_3)_2$ solution for at least 10 min and then placed in a H_2S-saturated aqueous solution with H_2S bubbling for 15 min. Loose ZnS/CdS particles were removed from the surface by copious washing in water, and, in the case of nylon and Nafion, by sonication. Sonication destroyed the Al_2O_3 films and removed the ZnS·CdS particles from glass and paper supports. Catalyst concentration and composition were determined by atomic absorption spectroscopy.

(*2*) *Catalyst Characterization.* The catalysts were examined by optical absorption spectroscopsy (the sample powder was diluted with silica powder and pressed into a thin pellet), X-ray diffraction (XRD), transmission electron microscopy (TEM, JEOL Model 200CX), and scanning electron microscopy (SEM, JEOL Model 35C). For TEM, the sample powder was first ground in an agate mortar and suspended in methanol (assisted by ultrasonication). This suspended liquid was pipetted over a carbon film microgrid and dried.

The surface composition was analyzed by X-ray photoelectron spectroscopy (XPS, Vacuum Generators ESCA LAB-II) equipped with an Al Kα radiation source. The Cd(3d)/Zn(2p) peak area ratio was used as a measure of the surface atomic ratio in the catalysts. Depth profiles were monitored by sputtering with Ar^+ ions for 2–10 min at an accelerating voltage of 9 kV and a beam current of 40 μA.

(*3*) *Photogeneration of Hydrogen from Water.* The photogeneration of hydrogen from water was carried out as follows: 50 mg of catalyst was placed on the bottom (not suspended) of a 19-mL Pyrex glass vial. Then 12 mL of 0.1 M Na_2S aqueous solution (pH 12.5) was added as a sacrificial reagent, followed by deaeration assisted by ultrasonication and a purge with N_2.

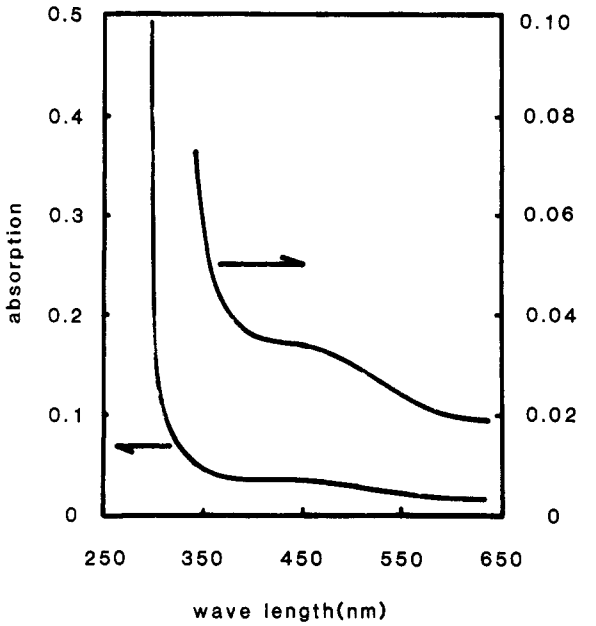

Figure 1. Absorption spectrum of $ZnS \cdot CdS/SiO_2$ catalyst.

TABLE I: XPS Analysis

	ratio of peak area (Cd/Zn)[a]	
catalyst	before sputtering	after sputtering
$ZnS(CdS/SiO_2)$	0.58	3.14
$CdS(ZnS/SiO_2)$	2.18	0.93
$ZnS \cdot CdS/SiO_2$	0.66	2.88

[a] Account has been taken of atomic sensitivity factors.[13]

A 450-W Xe lamp, with a water filter for removing IR light, was used to irradiate the catalyst through the bottom of the vial. The top of the vial was sealed with a rubber septum which allowed the removal of samples into a gas syringe for analysis. Products were measured by gas chromatography using a column packed with Porapak Q and N_2 was used as a carrier gas. After every sample removal the proper amount of N_2 was added to the vial to maintain a constant pressure of 1 atm.

For experiments with visible light a 440-nm cutoff filter (Corning 3-72) was used. More than 98% of the light with wavelengths shorter than 440 nm was eliminated by this filter. Quantum yields were measured with an Ar^+ laser with a wavelength of 488 nm.

Results

(*1*) *Characterization of Catalysts.* The absorption spectrum of the $ZnS \cdot CdS/SiO_2$ catalyst is given in Figure 1. There are strong increases in absorbance at 320 and 530 nm, near the bandgaps of ZnS (3.7 eV) and CdS (2.4 eV), respectively. This spectrum is clearly dominated by distinct ZnS and CdS features and there is no evidence of a solid solution. However, the $ZnS \cdot CdS/SiO_2$ catalyst showed a very broad XRD diffraction peak for ZnS and none for CdS, indicating that the average crystallite size in this catalyst was less than 2 nm. The XRD spectra of the unsupported ZnS·CdS catalyst indicated large crystallites of cubic ZnS and CdS.[11]

TEM showed that the unsupported ZnS·CdS catalyst contains large numbers of 200-nm particles. In the $ZnS \cdot CdS/SiO_2$ catalyst,

(11) "X-Ray Powder Data File", J. V. Smith et al., Ed., American Society for Testing and Materials, Philadelphia, PA, 1978, Card No. 5-566 and 10-454.

(12) J. J. Ramsden and M. Gratzel, *J. Chem. Soc., Faraday Trans. 1*, **80**, 919 (1984).

(13) D. Briggs and M. P. Seah, "Practical Surface Analysis by Auger and X-ray Photoelectron Spectroscopy", Wiley, New York, 1983, pp 511–514.

(14) M. F. Finlayson, B. L. Wheeler, N. Kakuta, K. H. Park, A. J. Bard, A. Campion, M. A. Fox, S. E. Webber, and J. M. White, submitted for publication.

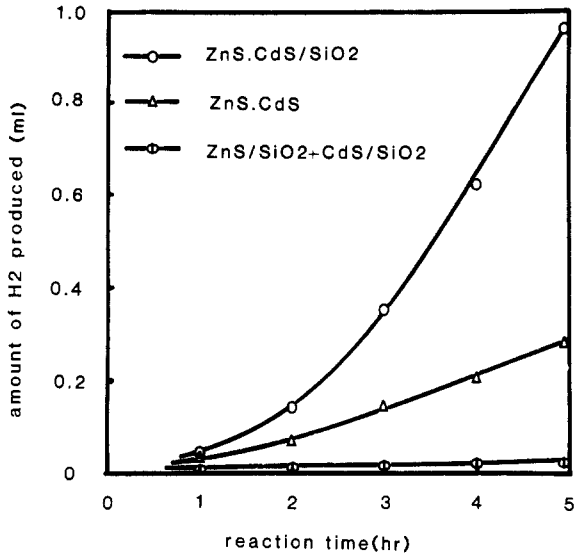

Figure 2. Amount of hydrogen produced by various catalysts under the irradiation with UV–visible light.

some coagulated particles (200 nm) were observed but the system was dominated by small sized particles (~10 nm). No coagulated sulfide particles were observed in a physical mixture of ZnS/SiO_2 and CdS/SiO_2 (particle size ~10 nm).

During the coprecipitation of ZnS and CdS over the surface of the SiO_2 powder, the concentrations of Zn^{2+} and Cd^{2+} ions in the liquid phase were monitored by atomic absorption spectroscopy. The Cd^{2+} and Zn^{2+} ions completely precipitated within 10 min; the Cd^{2+} ions precipitated a little more rapidly than the Zn^{2+} ions.

The ratios of XPS peak areas, Cd(3d)/Zn(2p), both before and after sputtering by Ar^+ are given in Table I for $ZnS{\cdot}CdS/SiO_2$, $ZnS(CdS/SiO_2)$, and $CdS(ZnS/SiO_2)$ catalysts. These results indicate that the outer surface is rich in Zn for both the $ZnS{\cdot}(CdS/SiO_2)$ and the $ZnS{\cdot}CdS/SiO_2$ materials while the reverse is true for the $CdS(ZnS/SiO_2)$ sample.

(2) Photogeneration of Hydrogen from Water. (a) UV-Visible Light Irradiation. No gases other than hydrogen were detected by gas chromatography during irradiation using either UV–visible or visible light. The amounts of hydrogen produced by UV–visible irradiation of $ZnS{\cdot}CdS/SiO_2$, unsupported ZnS·CdS, and the physical mixture of ZnS/SiO_2 and CdS/SiO_2 are shown in Figure 2. Only traces of hydrogen were observed when either a ZnS/SiO_2 and CdS/SiO_2 catalyst was irradiated separately. Figure 3 shows how the rate of hydrogen production varies with Cd/Zn ratio in coprecipitated $ZnS{\cdot}CdS/SiO_2$. (The amount of Zn was fixed.) The optimum ratio is near unity. When 50 mg of catalyst and a Cd/Zn ratio of unity were used, the weight percent of ZnS·CdS on the SiO_2 support was varied from 10 to 100%. There was no significant variation with loading in the range of 25–75 wt % but above and below these limits the rate dropped sharply to zero.

The amounts of hydrogen produced by the sequentially precipitated $ZnS(CdS/SiO_2)$ and $CdS(ZnS/Si_2O)$ catalysts during irradiation with UV light are compared with the $CdS{\cdot}ZnS/SiO_2$ catalyst in Figure 4.

Figure 5 compares the hydrogen production under UV–visible, visible, and dark conditions. Clearly, no hydrogen is produced in the dark. Figure 6 shows how the hydrogen production rate varies with the amount of $ZnS{\cdot}CdS/SiO_2$ catalyst employed. The monotonic decrease of the rate per milligram of catalyst indicates the importance of particle shadowing (i.e., many particles were, at most, only partially irradiated).

(b) Visible Light Irradiation. The H_2 production activities of $ZnS{\cdot}CdS/SiO_2$, $ZnS(CdS/SiO_2)$, $CdS(ZnS/SiO_2$, unsupported ZnS·CdS, and the physically mixed ZnS/SiO_2 and CdS/SiO_2 catalysts under visible irradiation are given in Figure 7. As for UV–visible irradiation, Figure 3, the variation of the rate with Cd/Zn peaked for Cd/Zn of unity. This result was obtained by either holding the CdS constant and varying ZnS or vice versa.

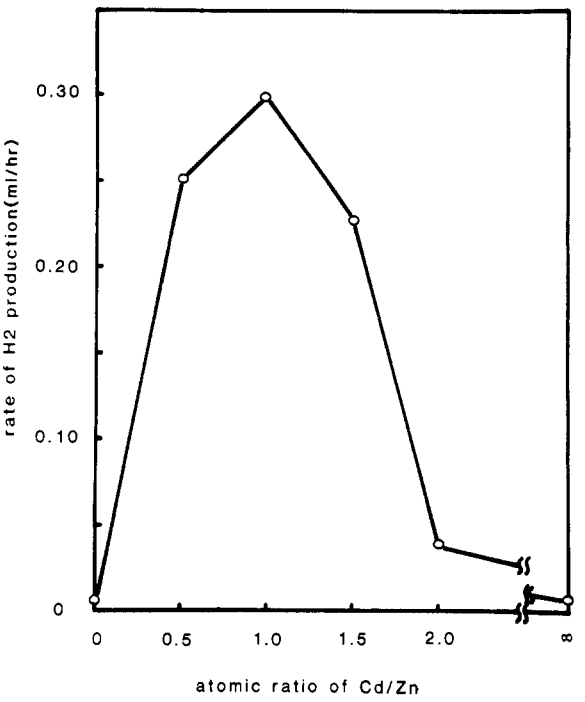

Figure 3. Effect of the atomic ratio of Cd/Zn on the rate of hydrogen production (UV–visible). The weight of ZnS was fixed and CdS varied.

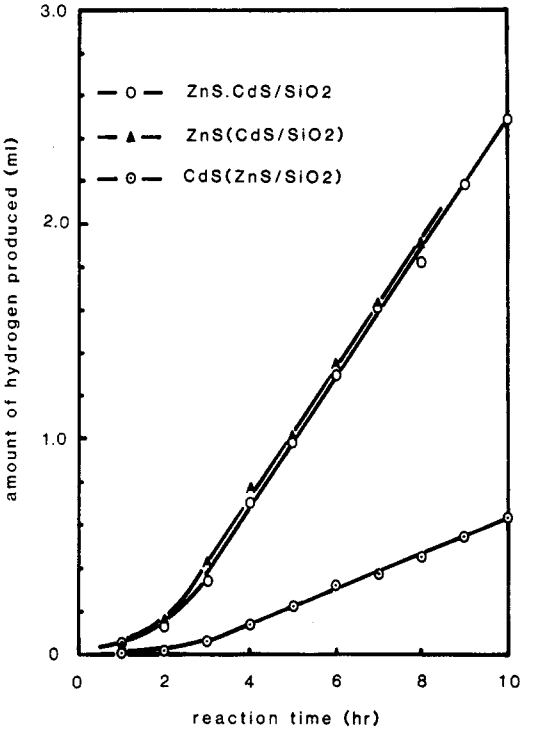

Figure 4. Amount of hydrogen produced by $ZnS{\cdot}CdS/SiO_2$, $ZnS{\cdot}(CdS/SiO_2)$, and $CdS(ZnS/SiO_2)$ upon irradiation with UV–visible light. The amounts of ZnS and CdS in these three catalysts were the same.

When the ZnS was fixed, the activity of hydrogen production decreased sharply with increasing Cd content above Cd/Zn = 1.0. The variation of Zn content with a fixed amount of Cd, above Zn/Cd = 1.0, had much less influence on the rate of hydrogen formation. The maximum quantum yield (moles of H_2/moles of photons) measured for $ZnS{\cdot}CdS/SiO_2$ catalyst with 488-nm light was 0.004.

(c) Other Supports. The steady-state rates of H_2 production for other supports with UV-visible irradiation are listed in Table II. As will be discussed below, the large activities of these other ZnS·CdS-supported systems are the result of less particle shadowing, not any fundamental chemical differences.

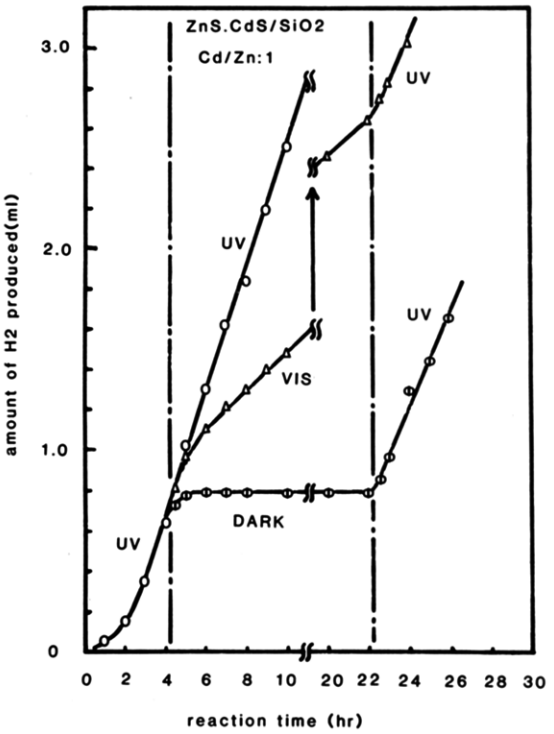

Figure 5. Change in the rate of hydrogen production (UV–visible, visible, dark). Catalyst was 50 mg of ZnS·CdS/SiO_2.

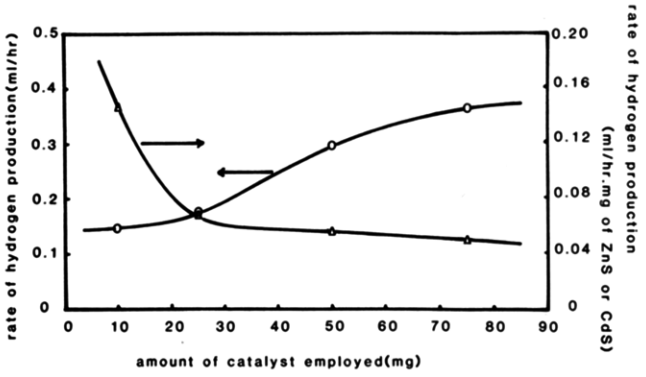

Figure 6. Variation in the hydrogen production rate (UV–visible) with the amount of ZnS·CdS/SiO_2 catalyst used.

TABLE II: Hydrogen Production from ZnS·CdS on Various Supports[a]

sample	support	mol of Cd/ mol of Zn	μL of H_2/h mg of CdS	relative rate
A	NAF 117	1	22.5	1.0
B	NAF 111	1	113	5.0
C	SiO_2	1	23.4	1.04
D	glass	8.9	293	13.0
E	weighing paper	1.5	369	16.4
F	colloids	0.77	760	33.7
G	nylon	1.4	500	22.2
H	Al_2O_3	1.3	650	28.9

[a] UV–visible irradiation.

Discussion

The structure, both microscopic and macroscopic, of the precipitated sulfides must be considered in discussing their hydrogen production activity. On the other supports (Table II), a significant increase (compared to SiO_2) is observed in all cases except Nafion, with the colloidal catalyst showing greatest activity. The colloidal particles, however, agglomerated after a few hours. Al_2O_3 is not a good support under these conditions because it slowly dissolves in the basic (pH 12.5) medium of the experiment. The Zn:Cd ratio was almost 1:1 in all cases except for the glass support.

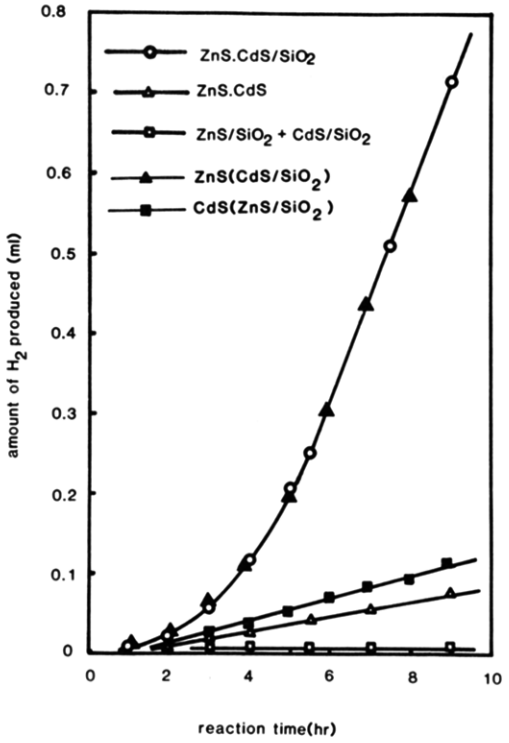

Figure 7. Amount of hydrogen produced by various catalysts with visible light.

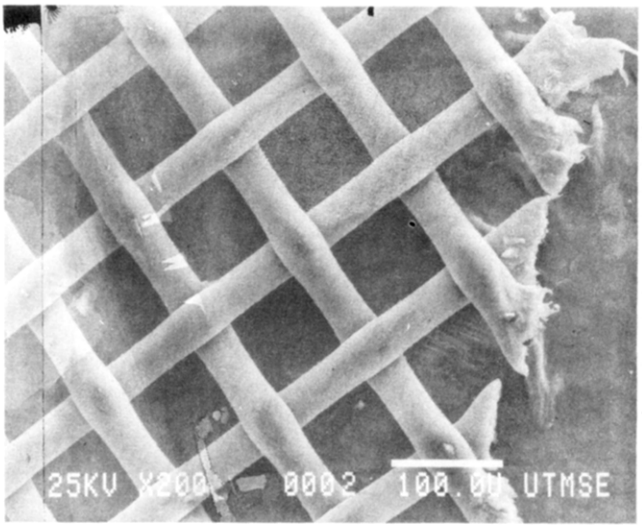

Figure 8. SEM of ZnS·CdS on nylon.

Interestingly, the morphology of the ZnS·CdS catalyst seems to exert a minimal effect on activity. For example, SEM studies of ZnS·CdS supported on glass, nylon, and Al_2O_3 reveal widely varying morphologies. Figure 8 shows the absence of large particles on nylon mesh and none were observed even at 10× higher magnification. The nylon mesh was yellow after ZnS·CdS treatment and presumably the catalyst uniformly coats the nylon strands. Figure 9 shows the cauliflower-like structure (no distinct particles) adopted by ZnS·CdS on frosted glass. SEM of the catalyst deposited on Al_2O_3 (Figure 10) shows clumps and individual particles with a diameter on the order of 0.3 μm. TEM of this system shows that these 0.3-μm particles are aggregates of ~40-Å-diameter particles. XRD of the Al_2O_3 supported catalyst indicates the presence of cubic ZnS and cubic CdS. In spite of these morphological variations, the activities are all within a factor of 2.

Since the H_2 production activity does not depend strongly on morphology, we must ask why the activity is so much larger on these supports than on the SiO_2- and Nafion-supported systems. The answer lies in the catalyst–light geometry. A very small

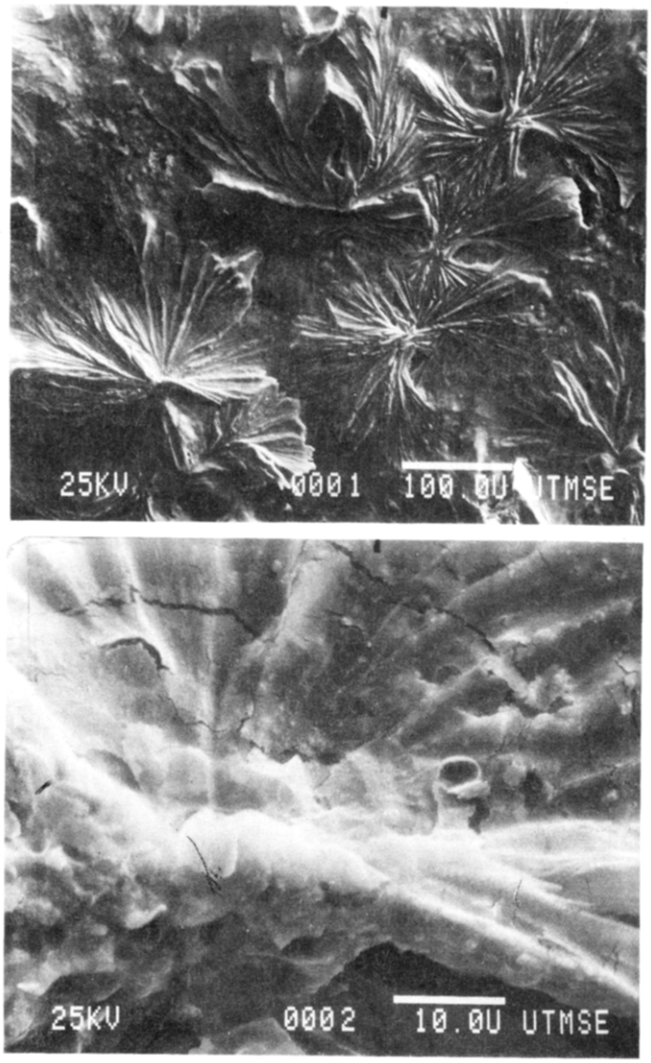

Figure 9. SEM of ZnS·CdS on frosted glass. The magnification of the bottom photo is 10× that of the top.

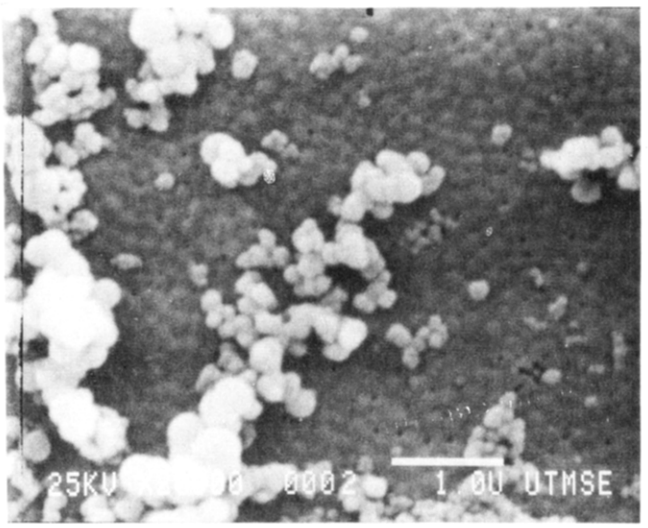

Figure 10. SEM of ZnS·CdS on Al_2O_3.

amount of catalyst was employed for samples D–H in Table II (≤0.2 mg) whereas the 50 mg of ZnS·CdS/SiO_2 typically employed for SiO_2-supported studies contains 28 mg of ZnS·CdS. Light scattering in the latter case substantially reduces the activity/milligram of catalyst. In effect, a large fraction of the catalyst is shadowed. To test this hypothesis, we irradiated smaller amounts of ZnS·CdS/SiO_2 (Figure 6); the activity per milligram of catalyst does indeed increase as the total amount of catalyst (and, therefore, light scattering) decreases. We conclude that the support, while greatly influencing macroscopic growth factors of the mixed ZnS·CdS catalyst, does not influence significantly the H_2 production activity.

Turning now to the SiO_2-based catalysts, the XPS data of Table I suggest that the coprecipitated mixed sulfide, ZnS·CdS/SiO_2, is similar to the sequentially precipitated sulfide, ZnS(CdS/SiO_2). The surface of these sulfides is clearly richer in ZnS than the subsurface region whereas the situation is reversed for the CdS-(ZnS/SiO_2). Thus, the ZnS·CdS/SiO_2 particles consist, to a first approximation, of an outer layer of ZnS and an inner layer of CdS. This is consistent with the thermodynamic solubility products of the two sulfides: 1.2×10^{-23} for ZnS and 3.6×10^{-29} for CdS, i.e., if kinetic factors can be neglected; as sulfide ion is added to the mixture, CdS precipitates first.

The H_2 production data of Figure 5 show that the ZnS·CdS/SiO_2 and ZnS(CdS/SiO_2) catalysts are a factor of 5 more active than CdS(ZnS/SiO_2). This result also points to the similarity of the coprecipitated catalyst and the sequentially precipitated ZnS(CdS/SiO_2).

The lower activity of the CdS(ZnS/SiO_2) can be understood in terms of the layered structure as follows. If we assume, as a structure–activity model, that H_2 production activity requires electron–hole pair formation near a boundary between ZnS and CdS, then an outer layer of CdS will suppress the rate because it absorbs both UV and visible light. In this view, the thicker the CdS layer, the poorer the H_2 production activity. On the other hand, an outer layer of ZnS will absorb only UV ($\lambda \leq 320$ nm) and thus visible light will penetrate to the CdS. With the layer model, the data in which the Zn/Cd ratio was varied can be rationalized as follows: (1) For Zn/Cd = 1, there is roughly one monolayer each of CdS and ZnS, *all* of the light is absorbed near a CdS/ZnS and solid–liquid interface and the activity is high. (2) For Cd/Zn = 2, much of the CdS layer is not covered by ZnS, so that a large fraction of the light absorbed is not near a CdS/ZnS interface and is not effective for producing hydrogen (this is supported by the similar hydrogen production rate under either visible or UV–visible radiation). (3) for Cd/Zn = 1/2 or 1/4, there is roughly one layer of CdS and two or four layers of ZnS. The observed activity is only slightly lower than that at Cd/Zn = 1. In this case visible light is still absorbed near an interface whereas UV light is absorbed further away than for the 1/1 system. The XRD data are not inconsistent with the layer-by-layer model presented here, since it does not necessarily involve the formation of detectable crystallites.

To provide perspective we note, however, that the amount of Cd^{2+} used (1.5×10^{-3} mol) would cover about 75% of the SiO_2 surface (~ 300 m^2 g^{-1}) with one layer of CdS if the coverage were uniform. Light absorption by such a layer would attenuate the visible or ultraviolet light by no more than 0.1%.[12] While this view is extreme, in the sense that there is no reason to expect perfect layer-by-layer growth, both here and in the Nafion case,[10] partial transmission of visible light was easily achieved (see Figure 1). These considerations point to additional reasons why Zn-rich exterior surfaces are important. One attractive possibility, presently being investigated, is that Zn^{2+} passivates surface states that are always present on precipitated CdS, thereby decreasing the electron–hole recombination rate and providing electrons of greater reducing power.

Conclusions

From this work the following conclusions are drawn:

Coprecipitated CdS·ZnS catalysts are active for H_2 generation with either UV–visible or visible light.

The activity is not strongly dependent on the support.

Sequentially precipitated (ZnS followed by CdS) catalysts are less active than either the reverse order sequentially precipitated or the coprecipitated catalyst.

XPS shows higher concentrations of ZnS on the surfaces of the more active catalysts.

Optical transmission of visible light through ZnS to the interface between ZnS and CdS and the exposure of Zn species to the

aqueous solution are important factors for achieving good activity.

Proximity of ZnS and CdS sites at the spatial location of optical absorption is also important for good activity.

Acknowledgment. The authors acknowledge financial support of this work by the Gas Research Institute (Contract No. 598-260-0756). National Science Foundation support of the X-ray photoelectron spectrometer by an equipment grant, CHE 8201179, is also acknowledged. We thank Dr. M. Schmerling for his help with the TEM and Prof. Marcin Majda and Cary Miller for supplying thin film samples of Al_2O_3.

Registry No. H_2O, 7732-18-5; H_2, 1333-74-0; CdS, 1306-23-6; ZnS, 1314-98-3.

Solvation Effects in Jet-Cooled 2-Aminopyridine Clusters: Excited-State Dynamics and Two-Color Threshold Photoionization Spectroscopy

James Hager and Stephen C. Wallace*

Department of Chemistry, University of Toronoto, Toronoto, Ontario M5S 1A1, Canada
(Received: February 28, 1985)

We present a detailed study of 2-aminopyridine and the 2-aminopyridine radical cation in a supersonic expansion. Dramatic changes in excited-state behavior have been observed upon the attachment of single solvent molecules. The solvent species investigated include Ar, CH_4, CCl_4, H_2O, MeOH, EtOH, NH_3, and 1,4-dioxane, which exhibit a wide range of excited-state interaction energies. Spectral features of the complexes were found to be quite rich in structure showing substantial vibrational excitation in the $\tilde{A}$ state especially for the polar solvent molecules. We also report a novel effect of complex formation on the excited-state dynamics of these complexes as inferred from measurements of fluorescence decay times. A considerable lengthening of the lifetimes of excited-state molecular complexes with polar solvents was observed and attributed to the ability of complex formation to affect the magnitude of the excited-state singlet–triplet interactions. In addition to these studies, we have also measured the IP's of the bare molecule and these complexes using the technique of two-color photoionization spectroscopy. The IP differences have provided information regarding the intermolecular interactions between a well-characterized molecular cation and neutral solvent molecules. Together with the spectral shifts of the uncharged species, these results clearly demonstrate the approximate order of magnitude increase in the stabilization of the 2-aminopyridine ground ionic level relative to the neutral excited state.

Introduction

The study of the solvation of aromatic molecules containing nonbonding electrons is particularly important in elucidating the interactions between two excited electronic states.[1-3] Nitrogen heterocycles are often characterized by two closely spaced electronic transitions, $n\pi^*$ and $\pi\pi^*$, leading to strong vibronic interactions manifested by complicated absorption spectra as well as easily perturbed radiative and nonradiative properties.[1,2,4]

We have investigated the behavior of 2-aminopyridine (2-AP) and a wide variety of its associated complexes of different interaction strengths in a supersonic jet. Condensed-phase studies[5-7] have demonstrated that even in hydrocarbon solvents 2-AP has an appreciable fluorescence quantum yield (~0.06 at 300 K) which is seen to increase by an order of magnitude in acidic solution. The rate constant for the radiative process was found to be independent of temperature and degree of protonation of the ring nitrogen while the nonradiative rate changes dramatically. An increase in the quantum yield of phosphorescence in nonpolar solvents relative to protic solvents at 77 K indicates a significant contribution of intersystem crossing to the nonradiative rate.[6] The change of fluorescence lifetime appears to closely follow the solvent-dependent fluorescence quantum yield.

In contrast to many of the recently studied nitrogen heterocycles such as quinoline, isoquinoline, and acridine which have lowest energy $n\pi^*$ singlet states, 2-aminopyridine is characterized[3] by a lowest energy π,π^* transition. However, many of the observable fluorescence properties are quite similar for these two groups of probe molecules. Those with a lowest energy $n\pi^*$ singlet state exhibit only a very weak fluorescence in hydrocarbon solvent while they show much more intense fluorescence in hydrogen-bonding solvents. This has been interpreted in terms of a greater energy gap between the $n\pi^*$ and $\pi\pi^*$ electronic states upon the formation of hydrogen bonds leading to a smaller vibronic interaction and a decreased nonradiative rate.[1]

Recently, Felker and Zewail[4] have demonstrated the important information that can be obtained from studying the interactions between the $n\pi^*$ and $\pi\pi^*$ states of isoquinoline via complex formation in a supersonic jet. In these investigations association with water, methanol, and acetone led to much longer fluorescence lifetimes than that of the bare molecule.[4b] This behavior was rationalized in terms of a change in the $n\pi^*$–$\pi\pi^*$ energy gap, depending on the complexing partner, decreasing the magnitude of the interaction between these two electronic states leading to a concomitant decrease in the nonradiative rate. The increase in the observed fluorescence lifetime reflects the strength of interaction of the particular solute species and its ability to form hydrogen bonds. Such direct information regarding solute–solvent interactions provides motivation for studying other molecular species and solvent partners in the unique environment of a supersonic expansion.

The lowest energy electronic transition of 2-aminopyridine has only recently been unambiguously assigned to a $\pi\pi^*$ electron promotion.[3] Thus, amino substitution of the parent pyridine molecule in this manner gives rise to substantially different excited electronic state dynamics as indicated by the significantly higher quantum yield of fluorescence exhibited by the 2-substituted molecule. Using a supersonic expansion to prepare rotationally and vibrationally cold 2-AP, we have investigated the fluorescence excitation and one-color multiphoton ionization (MPI) spectra of the bare molecule, extending the assignments of Hollas et al.[13] to approximately 2000 cm^{-1} above the origin. The formation of 2-AP complexes with polar and nonpolar solvent molecules results in distinct, sometimes complex, spectral features, which have been

(1) Lim, E. C. In "Excited States"; Lim, E. C., Ed.; Academic Press: New York, 1977; Vol. 3, p 305.
(2) Innes, K. K.; Byrne, J. P.; Ross, I. G. *J. Mol. Spectrosc.* **1967**, *22*, 125.
(3) Hollas, J. M.; Kirby, G. H.; Wright, R. A. *Mol. Phys.* **1970**, *18*, 327.
(4) (a) Felker, P. M.; Zewail, A. H. *Chem. Phys. Lett.* **1983**, *94*, 448. (b) Felker, P. M.; Zewail, A. H. *Chem. Phys. Lett.* **1983**, *94*, 454. (c) Felker, P. M.; Zewail, A. H. *J. Chem. Phys.* **1983**, *78*, 5266.
(5) Weisstuch, A.; Testa, A. C. *J. Phys. Chem.* **1968**, *72*, 1982.
(6) Kimura, K.; Takaoka, H.; Nagai, R. *Bull. Chem. Soc. Jpn.* **1977**, *50*, 1343.
(7) Kleinwachta, V.; Drobnik, J.; Augenstein, L. *Photochem. Photobiol.* **1966**, *5*, 579.

0022-3654/85/2089-3833$01.50/0